1988-26

RADON DYNAMICS IN A HOUSE HEATED ALTERNATELY BY FORCED AIR AND BY ELECTRIC RESISTANCE

Lynn M. Hubbard, Benjamin Bolker, Robert H. Socolow,
Center for Energy and Environmental Studies
Princeton University, Princeton, NJ 08544

Darryl Dickerhoff, Indoor Environment Group,
Lawrence Berkeley Laboratory, Berkeley, CA 94720

Ronald B. Mosley, Air and Energy Engineering Research Laboratory,
U.S. Environmental Protection Agency, Research Triangle Park, NC 27711

ABSTRACT

Understanding the various mechanisms driving radon entry into buildings aids in the development of appropriate diagnostic measurement techniques and in the design of efficient mitigation systems. Environmental parameters such as temperature, wind, and rainfall, and house specific parameters such as air exchange rate, type of heating and cooling system, and leakiness of the substructure to the soil gas provide the driving forces and conditions for radon entry. This paper presents field data and analysis which describe the effect of central heating air distribution systems, electric heating systems, and non-heating conditions on air infiltration into buildings, movement of air and radon around buildings, and the rate of entry of radon-containing soil gas.

This paper has been reviewed in accordance with the U.S. Environmental Protection Agency's peer and administrative review policies and approved for presentation and publication.[1]

I. INTRODUCTION

Several mechanisms are responsible for the time dependent variations in radon entry into buildings as a result of pressure driven flow. The dominant mechanisms are the "stack effect" (driven by temperature differences between the indoors and the outdoors), the effect of wind on the

---

[1]This work was funded in part by the Assistant Secretary for Conservation and Community Systems, Office of Building and Community Systems, of the U.S. Department of Energy under contract No. DE-AC03-765F0098.

building shell, and the operation of mechanical ventilation systems which distribute heated or cooled air throughout the house. The rate of radon entry into indoor air also varies with weather conditions, such as rain, which alter the soil conditions and thus the flow of soil gas through the soil to the building shell(1,2).

The Piedmont study conducted in New Jersey during 1986-87 and follow-up studies during 1987-88 have provided an extensive data set for deducing relationships between weather and house specific variables and radon behavior indoors(1,2). These relationships have contributed to the early stages of development and verification of a model which incorporates physical mechanisms for radon entry. The Piedmont data, however, are limited to forced-air heating systems. In order to clarify the role of the heating system, we performed research this past year at an additional house where we were able to vary the method of heating between forced air with a gas combustion furnace and electric resistance heating. This paper discusses the interesting relationships between radon entry and house dynamics which have emerged from this research.

We have two kinds of modeling efforts:

1. Heuristic modeling: a) to determine which house parameters are most important in driving radon entry, b) to determine if there is a house signature (some small set of quantities which are easy to measure) which can characterize the radon problem of the house, and c) to determine the extent to which soil gas entry varies from house to house.

2. Predictive modeling: a) to predict, given (by the modeling above) a few measured parameters from a house, the type of mitigation system best suited for the house, and b) to determine the relationship between short term and long term data; for example, can time series measurements taken in a house for one week in December be used to determine an annual average radon exposure?

These are long-term goals. The following discussion represents the results of a first step in this development process.

The paper is organized as follows. Section II describes the house and data used in this study, along with various techniques for estimating and measuring the radon entry rate, airflows, and radon concentrations in different parts of the house. Section III discusses the characteristic behavior of the radon and airflow dynamics during different types of heating periods. Section IV concludes with a discussion of an interzone flow model, with calculations of radon concentration and entry rate.

II. DATA COLLECTION

The data used in this study come from research house PU21. The house is a single-story ranch style house with a basement under one third of the

total floor area of the house and a slab under the rest of the house. The basement has hollow cinder block walls, a floor drain in the center of the basement slab, and a perimeter floor-wall crack.

The data consist of half-hourly measurements of temperatures indoors and outdoors, pressure differentials across the basement shell, heating system (HAC) use, outdoor weather station variables, radon concentrations at several points around the test house, and tracer gas airflow measurements. The temperature, pressure, and HAC measurements are part of our routine data collection at test houses, and are consistently available for all time periods. Continuous radon measurements are also routine for the basement, upstairs, and subslab, while wall radon measurements are intermittently available.

The airflow data come from a multiple tracer mass spectrometer (MTMS) system developed at Lawrence Berkeley Laboratory(3,4). The MTMS system emits different tracer gases in several zones, measures the concentrations of the gases in each zone, and uses a mass balance equation to calculate the flow between all zones and between zones and the outdoors continuously for specific time periods. The error in the MTMS data varies between the two heating periods used in this paper. During gas combustion, the average error was 2% for infiltrations and 10% for interzone flows, while during electric heat the errors were 8% for infiltrations and 15% for interzone flows. The error was always at least 5 m^3/hr for infiltrations and 10 m^3/hr for interzone flows(5).

Tracer gas emissions and concentration data can be used to calculate radon entry rates as well as airflows within houses. We have previously shown that, if we assume that the tracer gas emitted in the basement zone behaves the same as radon, the ratio of tracer gas emission to tracer gas concentration should be equal to the ratio of radon entry rate into the basement to radon concentration in the basement(6). Thus, knowing the tracer gas emission rate and concentration and the radon concentration in the basement, we can calculate the radon entry rate(6). The MTMS system can produce the data we need for this calculation.

III. VARIATIONS IN HEATING CONDITIONS

Research house PU21 was the site of experiments to compare the radon entry rate and the distribution of radon indoors during different heating conditions. The experiments involved heating the house alternately with electric resistance heaters installed on the living levels and with a gas combustion unit in the basement connected to a whole house air distribution system, sometimes called an air handler. The gas combustion furnace and air handler heating system usually runs on an automatic setback mode, during which the thermostat automatically sets back to 55°F (13°C) at midnight and turns back up to its previous setting at 8 AM. The data show that the air handler has a large effect on pressure differences across the building shell, and on the distribution of the radon indoors. We will compare these effects to the time periods when the air handler was not operating.

Figure 1 shows the radon concentrations, measured each half hour, in the basement and in the subslab during a gas combustion with automatic setback (GC) period along with the pressure differences between the outdoors and the basement and between the subslab and the basement, and the percent time the air handler is on during each half hour. Figure 2 shows the same parameters for an electric heat (EH) period. The sharp rise in the pressure differences coincides with the time the air handler is on. During this same time, the basement radon decreases while the subslab radon increases. Increased mixing of the basement air with the upstairs air by the air handler causes the decrease in basement radon concentration. The variation in the upstairs radon during the air handler use, not plotted in Figure 1, closely parallels the pattern of the subslab radon concentration, and the upstairs radon increases by roughly the amount of radon the basement loses.

Operation of the air handler is the main driving force for the variation in the radon concentration during GC. The air handler increases the pressure difference between the basement and the outdoors by 1.8 Pa, and between the basement and the subslab by 0.9 Pa. The increased pressure difference increases the air infiltration into the basement. This increased air infiltration includes both soil gas and outdoor air. Each house will have a different ratio between the degree of leakiness to the soil gas and the degree of leakiness to the outdoors. This ratio determines whether increased air infiltration raises or lowers the indoor radon concentration. It would be helpful to know how much this quantity varies among different houses. If it remains relatively constant among similar housing types on soils with similar permeabilities, it may be possible to design a measurement to characterize the potential radon problem on a building site based on the soil permeability and radon content. However, there is no indication in our research yet that the flow into buildings from the soil gas is similar in similar houses (6), although there are not yet many data to compare.

During the electric heating (EH) period, shown in Figure 2, the basement radon concentration lags the subslab radon concentration by about 2.5 hours, based on cross correlations computed at different lags. Regression analysis shows that the pressure differences (shown in the bottom plot) vary primarily because of the temperature difference between the indoors and outdoors, which causes a stack pressure of varying magnitude. A linear regression applied to the radon data from the EH period gives a good fit of the basement radon concentration ([Rn]) as a function of the radon in the subslab lagged 2.5 hours behind the basement radon, the temperature difference between the indoors and outdoors, and an intercept, or baseline radon concentration:

$$[Rn]_{basement} = 36\ (\pm 8)\ pCi/L + 0.10\ (\pm 0.003)\ [Rn]_{subslab,\ t-2.5\ hrs} + 7.7\ (\pm 0.5)\ pCi/L/^{o}C\ \Delta T$$

$$r^2 = 0.74$$

residual standard error = 42 pCi/L

A possible explanation for the 2.5 hour lag between subslab and basement radon is the relatively slow rate of convective flow from the subslab to the basement.

During the GC heating period, the best statistical fit for predicting radon in the basement, as a function of radon in the subslab, temperature difference between the indoors and the outdoors, and air handler time on, had a coefficient of determination (r^2) of only 0.17. The use of the air handler results in a perturbed, poorly correlated time variation of the basement and subslab radon concentrations.

Consider the time it takes for the subslab and basement radon to return to equilibrium--that is, a condition unaffected by the redistribution of basement air and increased basement air infiltration caused by the depressurization of the basement during air handler use. During the GC heating period, the air handler was off every night between midnight and 8 AM. Figure 1 shows that the basement radon concentration rises during these times while radon flow into the basement depletes the subslab radon. Figure 3 shows similar behavior in the wall; radon is depleted when the air handler is on and returns when the air handler shuts off. During the 8 hours that the air handler is off, though, the basement and subslab radon concentrations do not return to an equilibrium condition, as indicated by their failure to reach a condition where they are again statistically correlated with temperature difference and subslab radon concentration. In this house, therefore, the time it takes to return to equilibrium is longer than 8 hours.

The interiors of hollow block walls can be an important reservoir for radon (7), so it is important to understand radon behavior in walls under different heating conditions. Figure 3 shows wall radon concentrations at house PU21 during a 3-day period in the spring. Until day 97.375 (Julian day 97 at 0900), the HAC system stays off and the wall concentrations show a smooth daily cycle caused by the outdoor temperature cycle and the stack effect. When the HAC system comes on, it suddenly depletes the radon concentration in the walls. When it goes off the following night during setback, the radon concentration rises to its previous level or higher. During 2 days (Julian days 100 and 101) when the average outdoor temperature, 10.3 ^{o}C, was comparable to the non-heating period average outdoor temperature of 12.8 ^{o}C, the average wall radon level was 880 pCi/L, significantly higher than the non-heating period average of 530 pCi/L. Thus, the average wall radon concentration appears to rise during periods of HAC operation.

Table 1 presents averages of the measured data from house PU21 during the GC and EH heating periods. Both heating periods are during the middle of winter, with similar indoor and outdoor temperatures. This minimizes the difference in the contribution to indoor radon between the two periods due to the stack effect, so that the main difference between the two periods is the effect of the air handler on air and radon distribution, as discussed above. Table 1 shows the increased mixing of indoor air during GC; note the eightfold increase in basement to upstairs flow during the GC heating period and the two to threefold increase in upstairs to basement flow. Radon levels also indicate increased mixing during GC. The volume-weighted average of the radon concentration in the basement and upstairs increases

from 100 pCi/L during EH to 140 pCi/L during AS; in addition, the distribution of indoor radon changes. Much more radon remains in the basement during EH (302 pCi/L) than during GC (245 pCi/L). As a result, the upstairs radon concentration during GC (112 pCi/L) is a little more than double the amount during EH (51 pCi/L). Understanding how heating systems affect the distribution of the radon indoors is an important factor in determining how the health risk associated with exposure to radon varies between houses.

The radon entry rate, obtained as described in Section II using the emission rates and concentrations of the MTMS tracer gas, is higher during the GC period than during the EH period. Radon entry rate is a function of radon concentrations in the subslab and wall reservoirs around the basement and the flows from those reservoirs into the basement. HAC use depressurizes the basement, which both pulls radon from the surrounding soil into the subslab gravel bed and the interior of the block walls and increases the flow from those areas into the basement. Table 1 shows that average subslab radon concentration rises from 1460 to 2077 pCi/L during GC. Wall radon concentrations stay the same or rise slightly under HAC operation, as seen in Figure 3. Measuring flows from the soil gas reservoirs into the basement is quite difficult, but the 0.8 Pa increase in subslab-basement pressure differential and the 26 m^3/hr increase in basement infiltration, some of which represents soil gas, both indicate an increase in pressure-driven flow of soil gas into the basement. Decomposing the radon entry rate into a flow term and a concentration term by making more extensive flow and concentration measurements in the basement is a future project.

IV. ZONE MODEL

The flow model is a mass balance computer simulation of radon flow around a house. The model uses three zones to simulate radon flow between the basement, the upstairs, and the outdoors. The model also contains radon sources and sinks; therefore, the total amount of radon in the system can change over the course of time (unlike the system used to derive airflows from MTMS emissions data, where the amount of air in each zone and in the system remains constant). Outdoor air is a radon sink; the model assumes that it can absorb all the radon coming out of the house and still maintain a negligible radon concentration. The soil gas around the basement is the only radon source.

The flow model takes as input the measured flows between zones and the infiltration from outdoors every half-hour (a convenient time period), the initial radon concentrations in both zones, and an average entry rate into the basement. The model assumes the flows are constant over each half-hour period and that the radon entry rate is constant over the whole simulation period. The assumption of a constant entry rate is strong and somewhat inaccurate, as seen by the time variations in entry rate shown in Figure 4. The assumption is used for the sake of simplicity, and we will discuss in more detail below the associated error. The model predicts the radon concentrations in each zone for each half-hour by iterating the following

set of equations over short periods of time during which the radon concentrations in each zone are held constant (we have used 1 minute in this analysis, but we have also found that the whole-period average and the RMS error are not highly sensitive to iteration frequencies between 1 and 30 minutes).

$$[Rn(t)]_i \text{ (predicted)} = [Rn(t-1)]_i + [Rn(t)]_i\text{(inflow)} - [Rn(t)]_i\text{(outflow)}$$

where

$$[Rn(t)]_i \text{ (inflow)} = \frac{\Delta t}{vol_i} \times \left[\sum_j F(t-1)_{j \rightarrow i} \times [Rn(t-1)]_j + \dot{Rn} \right]$$

$$[Rn(t)]_i \text{ (outflow)} = [Rn(t-1)]_i \times \frac{\Delta t}{vol_i} \sum_j F(t-1)_{i \rightarrow j}$$

and where

i,j	index the different zones--basement, upstairs, and outdoors in this model;
$F(t)_{i \rightarrow j}$	is the flow from zone i to zone j during the time period from t-1 to t, in this case measured with the MTMS system;
$[Rn(t)]_i$	represents the radon concentration in zone i at time t;
vol_i	is the volume of zone i;
Δt	is the short time period during which radon concentrations in each zone are held constant; and
$\dot{Rn}$	represents a radon entry rate from outdoors, which is 0 except in the basement.

These equations neglect radon decay, which is very much smaller than the included terms. The inflow and outflow terms are on the order of 100 to 1000 pCi/L, while the decay term would be on the order of 1 pCi/L. The inflow and outflow terms are not actual measured concentrations; they are radon flows into or out of a zone, scaled by the zone volume to determine how they will change the radon concentration in that zone.

Figure 5 shows the model's output. The top plot compares measured and simulated radon concentrations in the basement while the bottom plot compares the measured and simulated concentrations upstairs, both for the 1-week MTMS flow measurement period. This simulation used soil radon entry rates calculated from the MTMS emissions data (see above, section II), 31 μCi/hr for the initial EH day and 37 μCi/hr thereafter. The general behavior of the modeled basement radon matches the measured radon fairly well; sudden peaks and drops in the measured radon concentration also appear in the modeled radon level. The simulated concentration varies more than the measured concentration, with higher peaks and lower troughs. The overall simulated average is slightly too high in the basement and slightly too low upstairs, predicting 287 pCi/L in the basement and 69 pCi/L upstairs as opposed to average measured values of 277 and 89 pCi/L, respectively. For the basement, the error of the average falls roughly within the 2% to 10% error of the flows. The RMS errors of 60 pCi/L for the basement concentration and 25 pCi/L for the upstairs during GC are somewhat greater,

at about 25% of the average levels. On the whole, however, the flow model predicts the average radon concentration quite well and the fine-scale behavior of radon reasonably well--especially given the assumption of a constant entry rate. Note that the model takes the measured radon concentration as input only once, at the beginning of the run; all radon concentrations are predicted beginning from the modeled concentrations of the previous time period. The relative success of the model in predicting radon concentrations indicates that the flow measurements are accurate, and that the model itself uses reasonable assumptions.

We have also modified the flow model to check the entry rates calculated from the MTMS emissions data. Instead of using the above equations iteratively to predict radon concentrations, the modified model takes the net predicted change in basement radon concentration, not including entry from the soil, and compares it to the change in measured radon over a half-hour period. Any shortfall in radon must be made up by entry from the soil, giving an entry rate for the period. (This analysis necessarily holds radon concentrations constant over the half-hour period, but the RMS error of the unmodified flow model discussed above increases only from 60 to 67 pCi/L when one makes this assumption by changing Δt from 1 minute to 30 minutes. Holding radon constant over 30 minutes, therefore, should not add too much error to the entry rate analysis.)

Figure 4 compares this modeled entry rate to the entry rate calculated from MTMS emissions data. Once again, the modeled and actual behaviors are very similar. The averages, 36.2 μCi/hr from the model and 36.7 μCi/hr from the emissions data, are again well within the experimental error of the flows, although the RMS error of 10.5 μCi/hr is high. The success of the model in matching the entry rates calculated in a different way provides a reassuring check of the validity of the assumptions used, both in constructing the model and in reducing the emissions data to airflow data. We could now reconstruct radon entry rates with some confidence from a set of interzone airflow and radon concentration measurements, without going back to raw emissions data which relate the tracer gas emission rate and concentration in the basement to the radon entry rate and concentration (as explained in section II). The flow model can estimate radon entry rates given radon concentrations and any set of airflow data, whether measured with tracer gas techniques or estimated in another way.

V. CONCLUSION

This paper has presented the distinct differences in radon and airflow behavior characteristic of two heating systems running in the same house. This comparison is particularly useful, because it allows an analysis of the effects of the heating systems while holding the other characteristics of the house constant. Radon distribution within the house, radon entry rate, and flows around the house have different behaviors under each heating system. This information is useful both on a practical level, in assessing radon concentrations and health risks in houses with different heating systems, and on a more scientific level, for understanding the characteristics of radon flow and general airflow in houses.

Along with the specific information about house dynamics, this paper has also introduced a number of analysis and modeling techniques. In particular, we have made preliminary attempts at deducing airflow and radon behavior around the house substructure. This behavior is very difficult to measure directly, and it is our hope that the flow model presented here will help to illuminate this behavior and check other results, as well as being the first step toward a more extensive macroscopic model of the movement of radon in and around houses.

VI. ACKNOWLEDGEMENTS

We thank Ken Gadsby of the Center for Energy and Environmental Studies, Princeton University, for his help, sensible advice, and participation in several useful discussions.

VII. REFERENCES

1. Dudney, C.S., Hubbard, L.M., Matthews, T.G., Socolow, R.H., Hawthorne, A.R., Gadsby, K.J., Harrje, D.T., Bohac, D.L., Wilson, D.L., "Investigation of Radon Entry and Effectiveness of Mitigation Measures in Seven Houses in New Jersey," mid-project report, ORNL/TM-10671, June, 1988.

2. Dudney, C.S., Hubbard, L.M., Matthews, T.G., Socolow, R.H., Hawthorne, A.R., Gadsby, K.J., Harrje, D.T., Bohac, D.L., Wilson, D.L., "Investigation of Radon Entry and Effectiveness of Mitigation Measures in Seven Houses in New Jersey," Final report (draft), ORNL-6487, September, 1988.

3. Dickerhoff, Darryl, Sherman, Max, Amarel, I., "Technical Description of the Multigas Measurement System," in preparation.

4. Sherman, Max, "On Estimation of Multizone Ventilation Rates from Tracer Gas Measurements," (Draft, LBL-25772).

5. Dickerhoff, Darryl, personal communication, September, 1988.

6. Hubbard, L.M., Gadsby, K.J., Bohac, D.L., Lovell, A.M., Harrje, D.T., Socolow, R.H., Matthews, T.G., Sanchez, D.C., "Radon Entry into Detached Dwellings: House Dynamics and Mitigation Techniques," accepted by Radiation Protection Dosimetry, 1988.

7. Hubbard, L.M., Bohac, D.L., Gadsby, K.J., Harrje, D.T., Lovell, A.M., Socolow, R.H., "Research on Radon Movement in Buildings in Pursuit of Optimal Mitigation," Proceedings of the ACEEE 1988 Summer Study on Energy Efficiency in Buildings, Asilomar, CA, 1988.

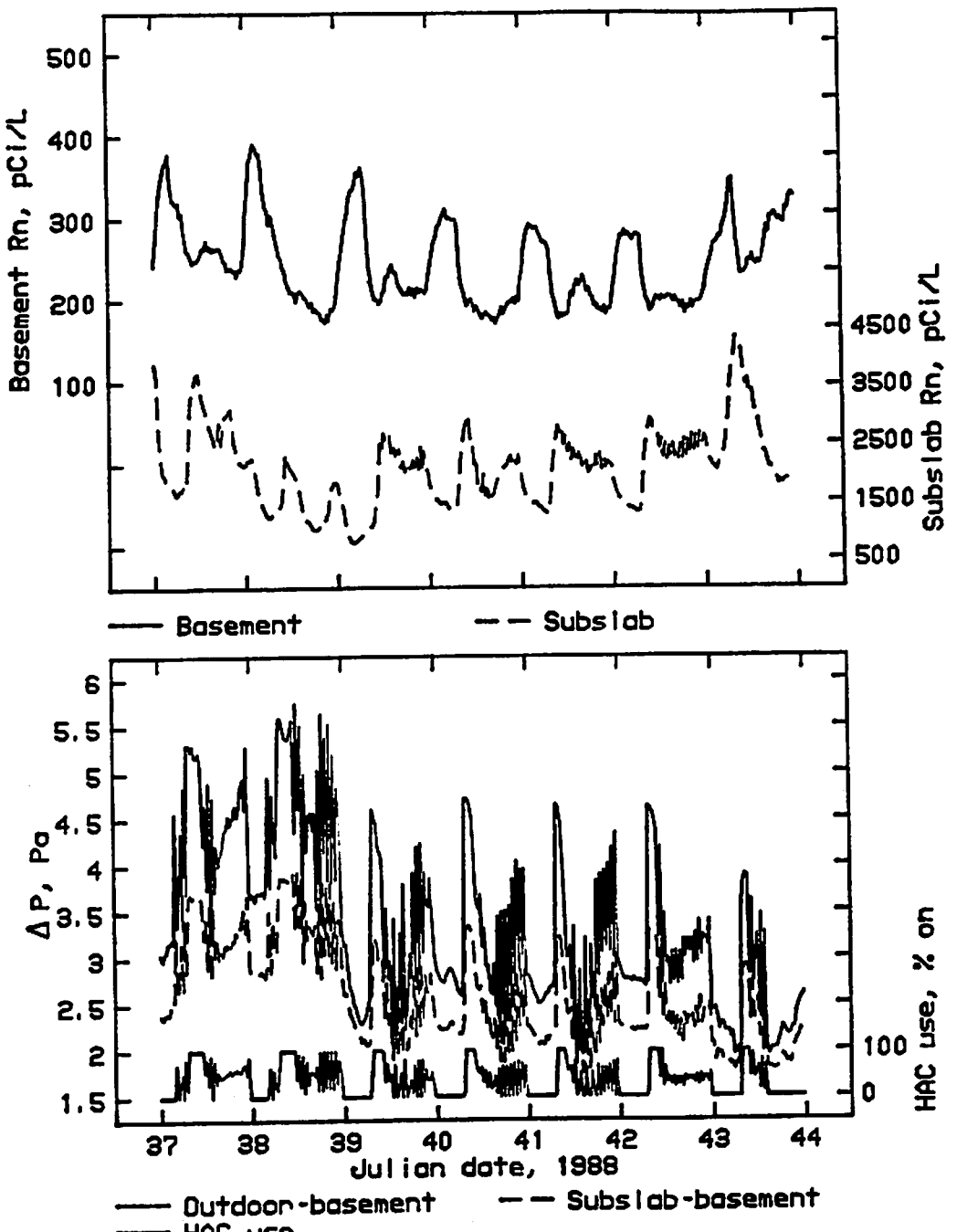

Figure 1. Radon concentrations, pressure differentials, and HAC use in house PU21 for a gas combustion/automatic setback (GC) period. The top plot shows radon concentrations in the basement (solid line) and below the basement slab (dashed line), in pCi/L (1 pCi/L = 37 Bq/m^3). The bottom plot shows pressure differentials in Pascals between the basement and the outdoors (solid line) and the basement and the subslab (dashed line); basement pressure is the reference. The solid line at the bottom of the plot shows what percent of each half-hour period the HAC system was running.

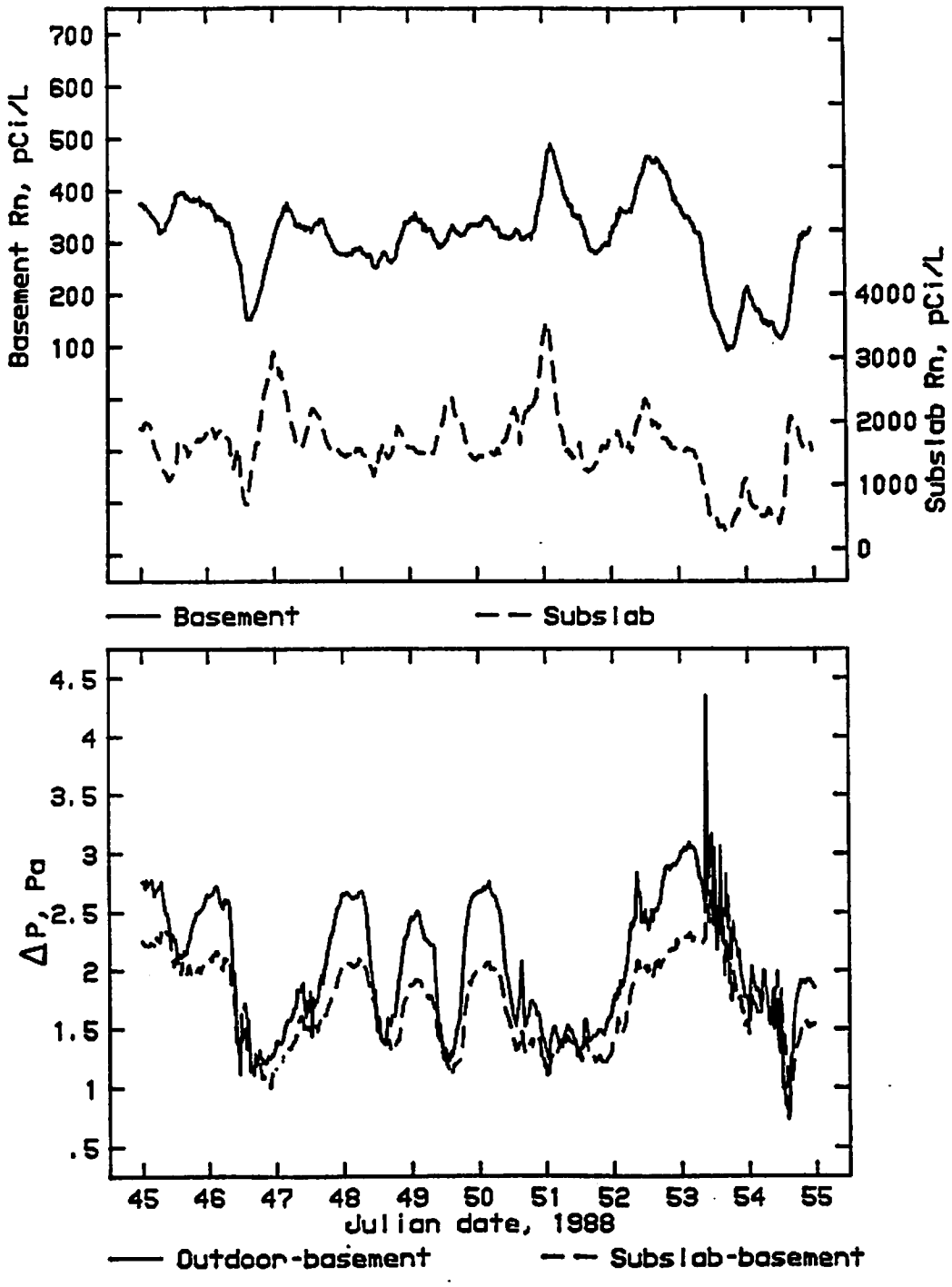

Figure 2. Radon concentrations and pressure differentials in house PU21 for an electric heat period. The top plot, as in Figure 1, shows basement and subslab radon concentrations in pCi/L. The bottom plot shows only pressure differentials in Pascals; the HAC system was off during this period. High winds (10-15 mph, or 4.5-6.7 m/s) on days 53 and 54 caused the pressure spike shown on the bottom plot.

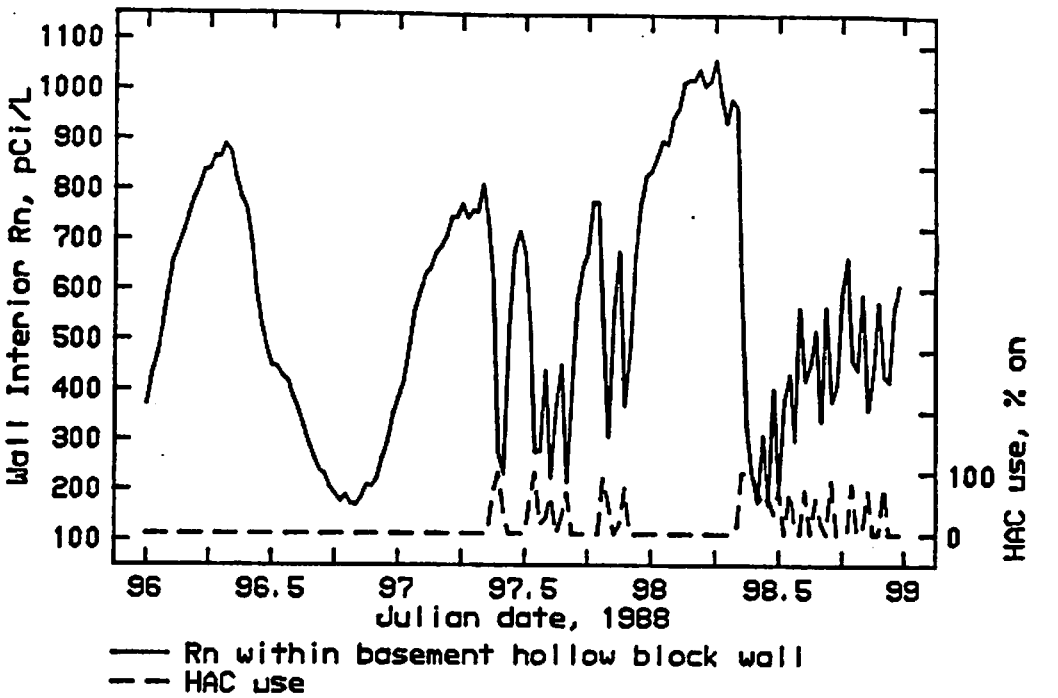

Figure 3. Radon concentrations within the basement hollow block wall (solid line), in pCi/L (1 pCi/L = 37 Bq/m^3), and HAC use (dashed line), in percent time on, at house PU21.

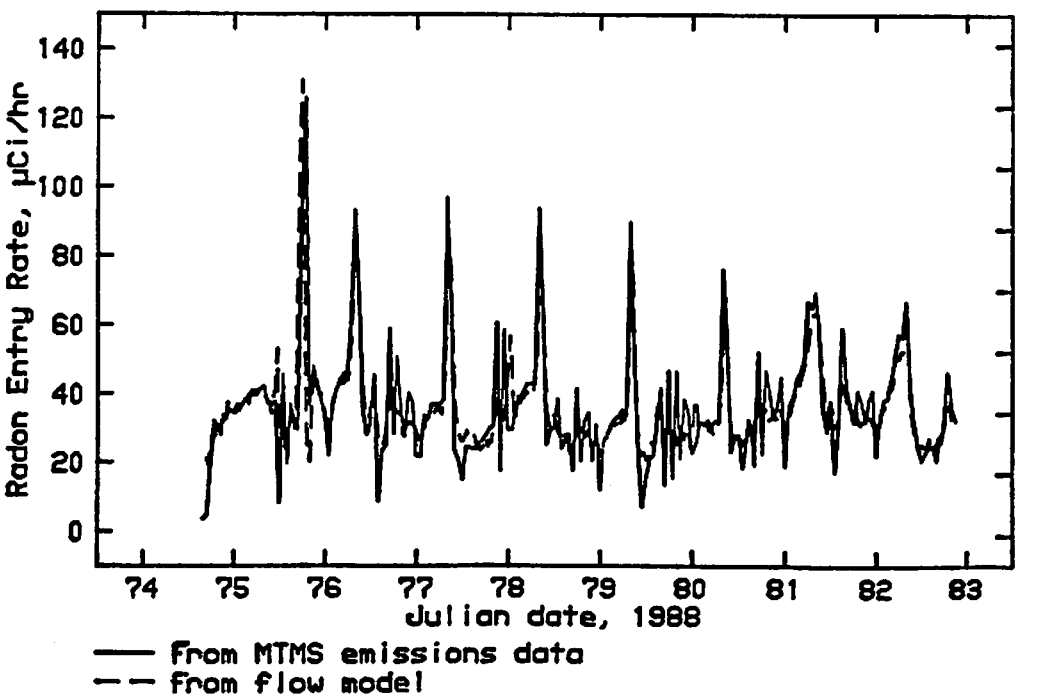

Figure 4. Radon entry rate from soil gas into the basement of house PU21 as calculated from MTMS emissions data (solid line) and from the flow model using MTMS flow data (dashed line), in µCi/hr (1 µCi/hr = 37 kBq/hr).

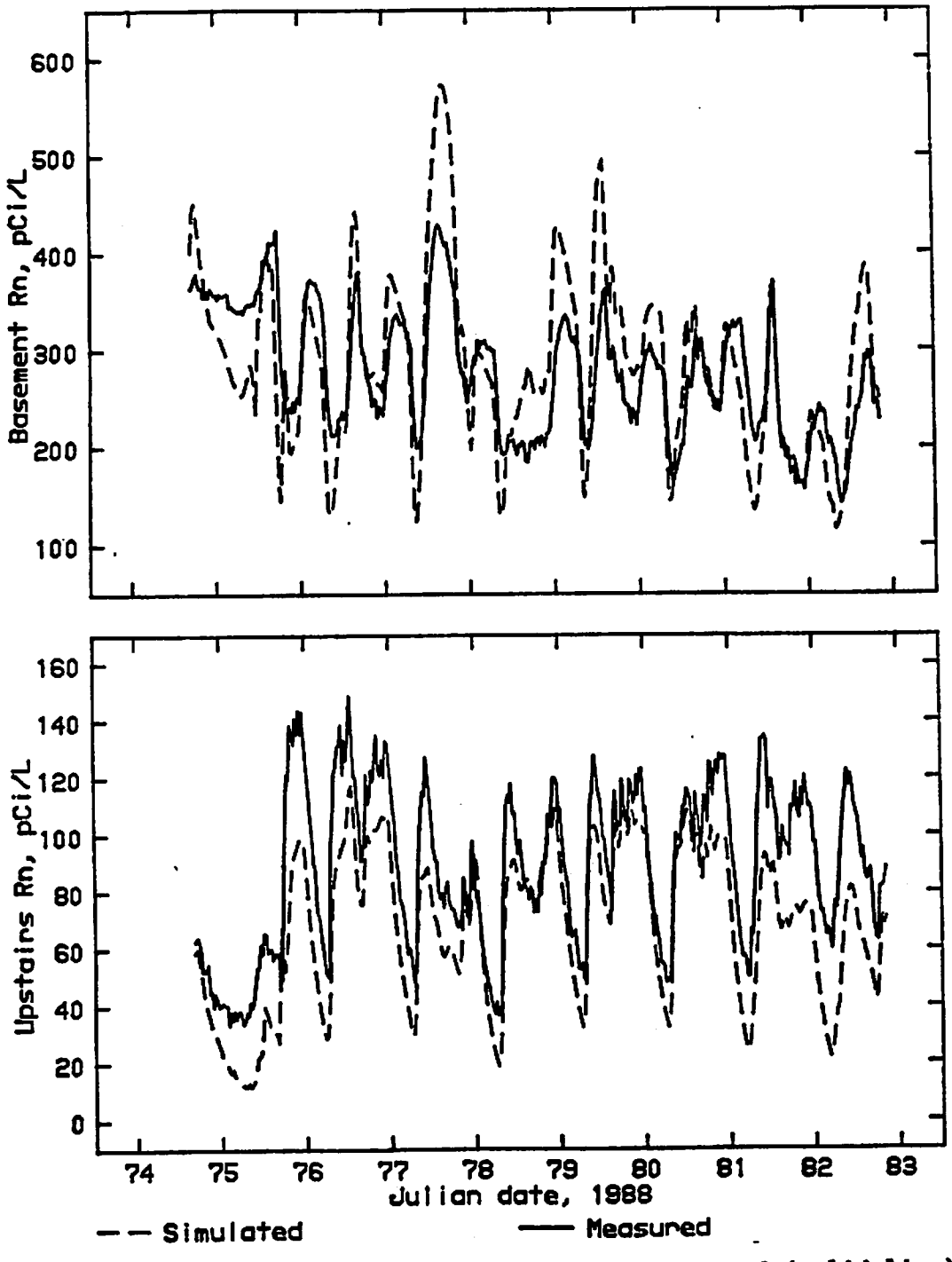

Figure 5. Radon concentrations in house PU21 as measured (solid line) and as simulated by the interzone flow model (dashed line), using MTMS airflow data, an estimated constant source strength of 31 μCi/hr during electric heat and 37 μCi/hr during GC, and initial radon concentrations as measured at the beginning of the period. All concentrations are in pCi/L (1 pCi/L = 37 Bq/m^3). The top plot shows basement concentrations, the bottom plot shows upstairs concentrations.

Table 1. Heating periods at House PU21: averaged measured quantities.

	electric heat	gas combustion/ automatic setback
Julian days	74.8-75.8 [45-55]*	75.7-82.7 [37-44]
Zone volumes: (m^3)		
basement	118.5	
upstairs	467.1	
Radon concentration: (pCi/L)†		
[Rn], basemen	[302]	[245]
[Rn], upstairs	[51]	[112]
[Rn], subslab	[1460]	[2077]
[Rn], whole house (volume-weighted average)	[102]	[139]
Pressure differences: (Pa)		
outdoors-basement	[2.19]	[3.39]
subslab-basement	[1.80]	[2.60]
upstairs-basement	[0.16]	[0.85]
HAC system use: (percent on)	0	[34.7]
Entry Rate: (μCi/hr)		
from MTMS data	31.9	37.4
Flows: (m^3/hr(ACH))		
Infiltration-		
basement	67(0.57)	93(0.78)
upstairs	132(0.28)	147(0.31)
basement to upstairs	10	80
upstairs to basement	33	87
Temperature: (^oC)		
basement	[14.9]	[20.9]
upstairs	[17.8]	[18.6]
outdoors	[1.54]	[-2.0]

* Days in brackets ([]) are alternate periods from which more data were available; quantities in brackets are taken from these periods.

† 1 pCi/L = 37 Bq/m^3